Impact of Capacitor Voltage Transformers on Phasor Measurement Units Dynamic Performance

Roberto Ferrero*, Paolo Attilio Pegoraro†, Sergio Toscani‡

*Department of Electrical Engineering and Electronics
University of Liverpool, Liverpool, United Kingdom
Email: roberto.ferrero@liverpool.ac.uk

†Department of Electrical and Electronic Engineering
University of Cagliari, Cagliari, Italy
Email: paolo.pegoraro@diee.unica.it

‡Dipartimento di Elettronica, Informazione e Bioingegneria
Politecnico di Milano, Milan, Italy
Email: sergio.toscani@polimi.it

***Abstract*—Measurements of synchronized phasors, frequency and rate of change of frequency from different locations on a wide area are the outputs of phasor measurement units (PMUs), which enable a frequent and accurate monitoring of power systems. PMUs have been conceived for monitoring ac transmission systems; in this case, they process the measurement signal provided by transducers that may have a strong impact on the overall performance. Capacitor voltage transformer represents one of the most widely employed transducer in high-voltage applications. In this paper, its effects on the response to amplitude and phase step signals of different, well-known PMU algorithms are investigated through numerical simulations. The paper proves that standard PMU characterizations or compliance verifications are not capable to identify the overall dynamic behavior of the device when installed on the field. Therefore, considering the effect of the transducer is a mandatory step towards the definition of measurement specifications for actual applications.**

Keywords*—*phasor measurement unit (PMU), power transmission, transducer, capacitor voltage transformer, synchrophasor estimation, frequency.

I. Introduction

Phasor Measurement Units (PMUs) provide measurements of synchronized phasors, frequency and Rate of Change of Frequency (ROCOF) in power networks and are intended to guarantee a frequent and accurate monitoring of power systems. PMUs may be conceived for different applications and thus their design can be optimized for different performance goals. In this respect, the standard IEEE C37.118.1 [1] identifies two main applications, thus defining two corresponding performance classes: P class is devoted to protection applications requiring fast responses and low latency, while M class is meant to provide high measurement accuracy under steady-state conditions. For these reasons, the synchrophasor standards ([1] and [2]) introduce test scenarios to verify the PMU behavior under both steady-state and dynamic conditions, while defining limits for measurement errors and parameters to evaluate the dynamic response.

In recent years, an intense research activity have taken place about algorithms for PMUs (see [3] for a review of possible approaches and methodologies for algorithm design). The different techniques have been carefully compared using the test conditions of the standards under simulation [4], [5]. In [6] reference algorithms for PMU characterization under different conditions have been presented. Other approaches aim at the an experimental characterization of the algorithms when running on actual devices, while providing a comparison to simulation results [7]. In [8] a full experimental testbed aimed at comparing PMU algorithms in a realistic scenario is proposed.

In this paper the focus is shifted to the typical measurement chain of a PMU installed in a transmission network and, in particular, to the impact of the voltage transducer on the overall performance. Capacitor Voltage Transformers (CVTs) represent the most widely employed voltage transducers in transmission systems. They are based on the connection of a capacitive voltage divider and a potential transformer through a compensation reactor. By properly tuning the inductance of this reactor, a virtually negligible phase shift between the input of the voltage divider and the secondary voltage of the transformer is achieved at the rated frequency. However, the well-known drawback is a severe bandwidth limitation that results in poor transient performance. For this reason, the impact of CVT dynamics on protective relays [9] and harmonic measurements [10] has been studied for a long time. Such analyses are based on proper equivalent circuit models of the CVT [11] experimentally validated by frequency response measurements [12].

More recently, the impact of the transient performance of CVTs on phasor measurements has been investigated [13]. Estimation techniques able to reduce the detrimental effect of their slow, underdamped dynamics have been proposed in the literature [14], [15]. However, these works does not analyze how the behavior of the CVT may significantly affect the results of the accuracy tests for PMUs ruled by [1].

This paper investigates the impact of CVTs on the most severe dynamic tests required by [1], namely the amplitude and phase angle step tests. The transducer behavior is represented by means of a transfer function model. The test signals are applied to its input, while its output is fed to different, well-known PMU algorithms. The dynamics of the resulting measurement errors are investigated by simulation using the standard total vector error (TVE), frequency error (FE) and ROCOF error (RFE) thus showing the overall system response.

II. Dynamic Model of the CVT

As explained in the introduction, the CVT represents the typical voltage transducer employed in high voltage transmission grids. Basically it consists of a capacitive divider connected to the voltage to be monitored which feeds, through a properly tuned inductor, the primary winding of a voltage transformer; its secondary winding provides the voltage signal for measuring instruments and relays, that represent the burden. Using such a voltage divider for obtaining some part of the required step-down ratio allows a better design of the step-down transformer, since it helps solving insulation issues. In turn, the transformer guarantees the galvanic separation between power system and secondary circuit, as required for safety reasons. The series inductor is tuned according to the output capacitance of the divider and the equivalent inductance measured at the primary side of the step-down transformer so that, at the rated frequency, the voltage at the secondary side of the transformer is in phase with the line voltage applied to the capacitive divider.

This operating principle is extremely effective for steady-state voltage measurements at the rated frequency; however, being based on a inductor-capacitor resonance produces a severe bandwidth limitation and in general a poor dynamic behavior. The result is that fast voltage transients may be severely distorted by the filtering behavior of the transducer. Furthermore, the interaction between the output capacitance of the divider, the inductance of the tuning reactor and the iron core of the step-down transformer makes this devices prone to ferroresonance phenomena under particular conditions. When the burden itself does not provide sufficient damping, a ferroresonance suppression circuit (FSC) is introduced at the secondary side of the transformer. FSCs can be classified in passive or active. Passive FSCs consists of a resistor that may be permanently connected or as long as an overvoltage transient is detected. Active FSCs are made of capacitor and inductors which are permanently connected in parallel to the burden and tuned to the rated frequency; it becomes clear that they considerably modify the transient behavior of the CVT.

Analyzing the impact of CVTs on the accuracy of synchrophasor, frequency and ROCOF estimation algorithms under dynamic conditions requires a proper mathematical modeling of the transducer. In this respect, several dynamic models of CVTs can be found in the literature. According to the purpose, some of them include a nonlinear representation of the iron core, the stray capacitances of the voltage transformer winding, the FSC, etc... In this work, the model of a 60 Hz CVT employed in [14] is considered. The equivalent circuit is shown in Fig. 1; the parts representing the capacitive divider, the compensating inductor, the step-down transformer, the FSC and the burden are indicated. The values of the parameters are listed in Table I.

It should be noticed that the voltage transformer has been modeled with the usual Steinmetz equivalent circuit, but the branch considering the magnetizing current has been removed. In fact, its effect is usually negligible for small and fast voltage variations as those considered in this work. However, in this way ferroresonance phenomena are not considered, but they are not likely to occur thanks to the active FSC included in the model. Furthermore, the stray capacitances of the windings have not been modeled; the reason is that their effect appears at frequencies of few kilohertz, therefore well above the typical bandwidth of PMU algorithms.

TABLE I. Parameters of the CVT model

Parameter	Value
R_1	3310.7 Ω
C_1	1.605 nF
R_2	59.0338 Ω
C_2	89.991 nF
R_{LE}	950.06 Ω
L_{LE}	72.724 H
R_{PE}	850.02 Ω
L_{PE}	4.4433 H
R_{SE}	246.7 mΩ
L_{SE}	649.91 μH
K	5058/66.7
R_F	13.333 Ω
R_{CF}	80 mΩ
C_F	165.36 μF
R_{LF}	1.2301 Ω
L_F	54.3 mH
R_O	29.551 Ω
L_O	98.2 mH

The linear relationship between the secondary and the primary voltage (v_2 and v_1 respectively) resulting from the equivalent circuit is expressed by the transfer function $H(s)$. It comprises six poles (including two complex conjugate pairs) and five zeros (two at the origin and a complex conjugate pair). The compensating inductor is tuned so that the frequency response function $H(j\omega)$ assumes the real value C at the rated frequency $f_0 = 60$ Hz. This value is employed to obtain $v_{1,r}$, namely the reconstructed primary voltage; in the Laplace domain it results:

$$V_{1,r}(s) = \frac{1}{C} H(s) V_1(s) = M(s) V_1(s) \qquad (1)$$

where $V_{1,r}(s)$ and $V_1(s)$ are the Laplace transforms of $v_{1,r}$ and v_1, respectively.

III. Tests and Results

A. Test Assumptions

The test signals defined in the synchrophasor standard [1] to measure the step response of a PMU have been adopted as primary voltages waveforms. In this paper, only single-phase tests has been considered. The primary voltage signals can be described as follows (using a continuous-time notation):

$$v_1(t) = A(1 + k_x 1(t - t_0)) \cdot \cos(2\pi f_0 t + \phi_0 + k_a 1(t - t_1)) \qquad (2)$$

where A is the signal amplitude, f_0 is the rated frequency, ϕ_0 is the initial phase angle. k_x and k_a are, respectively, the amplitude and phase-angle step sizes, $1(t)$ is the unit step

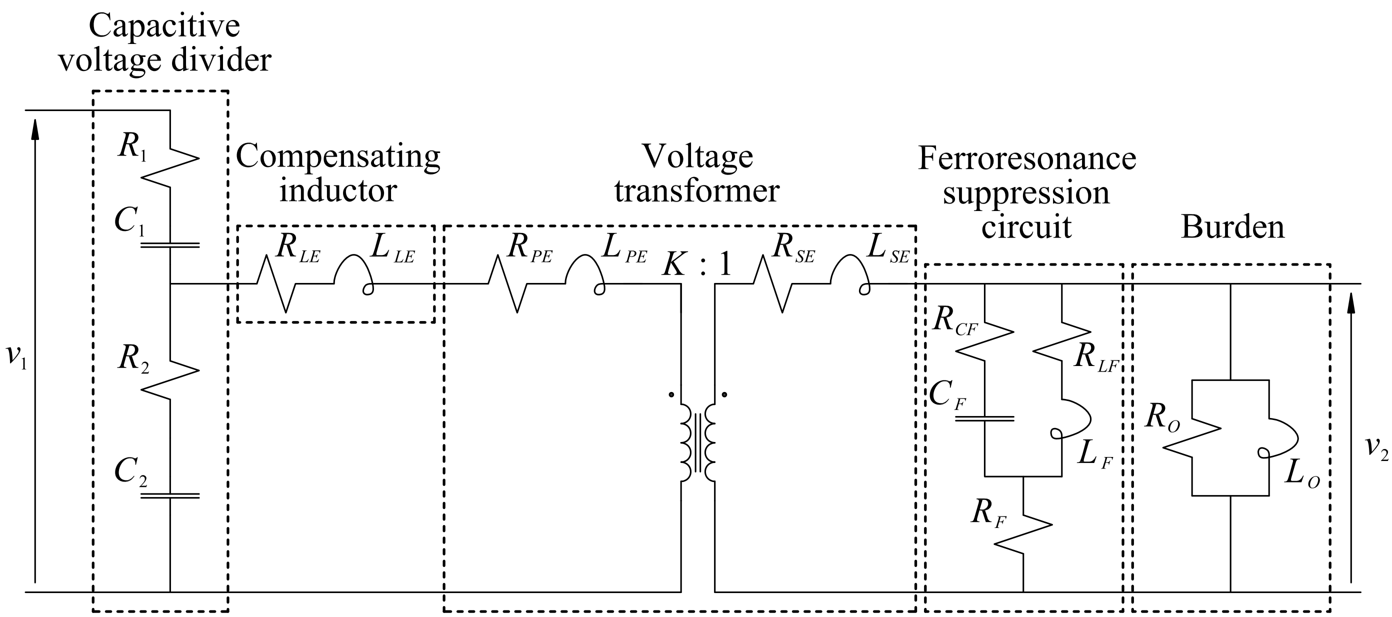

Fig. 1. Equivalent circuit employed to model the CVT.

function, while t_0 and t_1 are the step application instants. The following values have been used in the tests:

- Common values: $f_0 = 60\,\mathrm{Hz}$, $A = 1\,\mathrm{p.u.}$, $\phi_0 = 0\,\mathrm{rad}$. The duration of the tests is $2\,\mathrm{s}$.
- Amplitude step test: $k_x = +0.1$, which corresponds to a $10\,\%$ amplitude increase, $t_0 = 0.5\,\mathrm{s}$, $k_a = 0$ and t_1 irrelevant.
- Phase angle step test: $k_a = +10^\circ$ ($0.1745\,\mathrm{rad}$), which corresponds to an instantaneous positive variation of the phase angle, $t_1 = 0.5\,\mathrm{s}$, $k_x = 0$ and t_0 irrelevant.

In all the tests, three algorithms have been compared to explore possible differences in their behavior. Since P-class algorithms are specifically designed to have a fast step response, the following three configurations, based on a two nominal cycles observation window, have been used:

1) Standard P-class algorithm (P-C37118 in the following): it is the algorithm suggested by the standard [1, Annex C] based on a complex mixer (to achieve a frequency shift towards baseband) and a low-pass finite impulse response filter whose coefficients corresponds to a two-cycle triangular window.
2) Interpolated DFT (IpDFT) with a two-cycle window (2 IpDFT): it is a classic algorithm based on discrete Fourier transform (DFT), where frequency is estimated as a function of the ratio between the two largest DFT bins. Amplitude is then obtained by compensating the possible scalloping loss due to off-nominal frequency (e.g., see [16]). A Hann window is employed in the following.
3) Taylor Fourier filter (2 TF): the method, proposed in [17] is based on a second order Taylor expansion of the phasor around the measurement instant. Frequency and ROCOF are computed from the first and second order derivatives of the phasor.

B. Test Results

For each test, the step-changing signal $v_1(t)$ is generated (with sampling rate $f_s = 12\,\mathrm{kS/s}$, corresponding to 200 samples per cycle) and used as an input of the dynamic system $M(s)$ modeling the voltage measurement process. The resulting output $v_{1,r}$ is then forwarded to all the algorithms to compute the synchrophasor, frequency and ROCOF values. All the computations are performed on a per-sample basis and, in the same time instants, they are compared with those obtained by considering an ideal transducer. Therefore, in this case, the PMU algorithm is directly fed with an ideal amplitude or phase step signal.

First of all, the amplitude step test is considered. Fig. 2 shows the instantaneous error between the actual instantaneous primary voltage and its reconstructed value by using the transducer output and its gain at the rated frequency. The effect of the delay introduced by the transducer and the oscillations produced by its modes are clearly visible.

Fig. 3 shows the evolution of the synchrophasor amplitude around the measurement point for the three algorithms when the transducer dynamics is considered or not (the response after the step is zoomed in the inset box). Except for the very first time instants, the P-C37118 and 2 IPDFT algorithms seem to be only weakly affected by the voltage transformer. Among the considered algorithms, the 2 TF is the one having the fastest dynamic response. This characteristics makes the impact of the transducer more evident: a longer transient showing an oscillatory behavior due to the conjugate pole pairs that characterize the transfer function can be clearly noticed. In fact, the response is the result of the step distortion introduced by the transducer dynamics that is only partially masked by the filtering behavior of the specific estimation algorithm. This effect is much more pronounced for the frequency estimation, as reported in Fig. 4. In this case, not only TF algorithm but also P-C37118 and 2 IPDFT show large oscillations before the frequency settles. The errors before and after the transition are

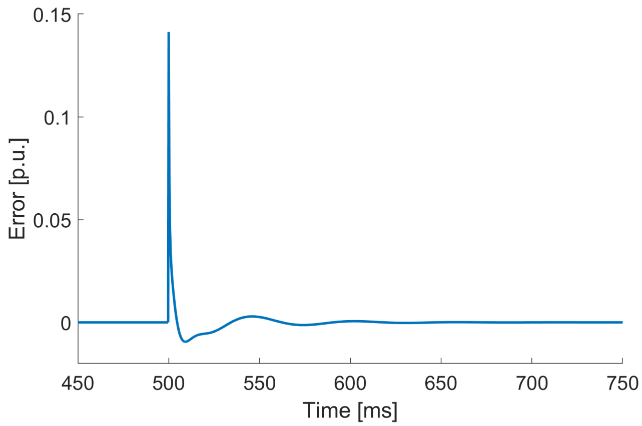

Fig. 2. Amplitude step test, deviation between actual and reconstructed primary voltage.

zero but the transient can be quite long, especially for the 2 IPDFT that in this case exhibits the largest and less damped oscillations.

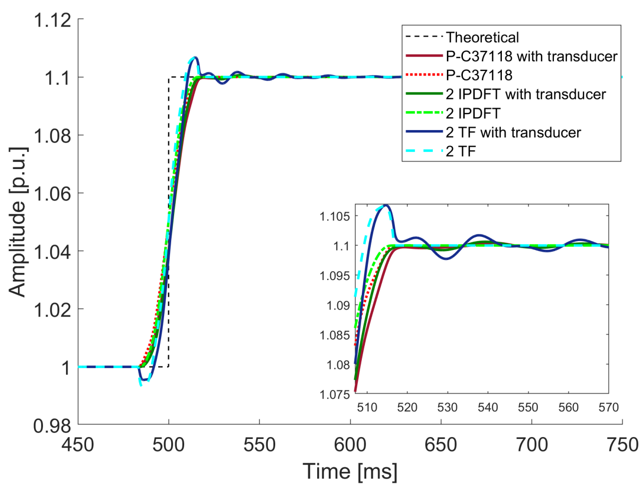

Fig. 3. Amplitude step test, amplitude estimation.

Table II shows the response time of both phasor and frequency estimations and overshoot values in the above case. Response times are computed as defined by [1], that is by calculating the time during which the estimates are outside the limits for measurement errors under steady-state conditions (TVE $= 1\,\%$ and FE $= 5\,$mHz for phasor and frequency, respectively). Overshoot values clearly depend on the amplitude of the perturbation, thus they are reported as a percentage of the step size. The results show that the transducer increases the transient duration. This is also due to the filtering effects of the transducer but, to a greater extent, to the modes of its step response, as illustrated in Section II. Overshoot and undershoot increase or even appear when the algorithm presents a purely monotonic step response (e.g. P-C37118), however their values are similar to those obtained without considering the transducer dynamics.

Fig. 5 reports the difference between the actual primary voltage and its reconstruction from the CVT output when

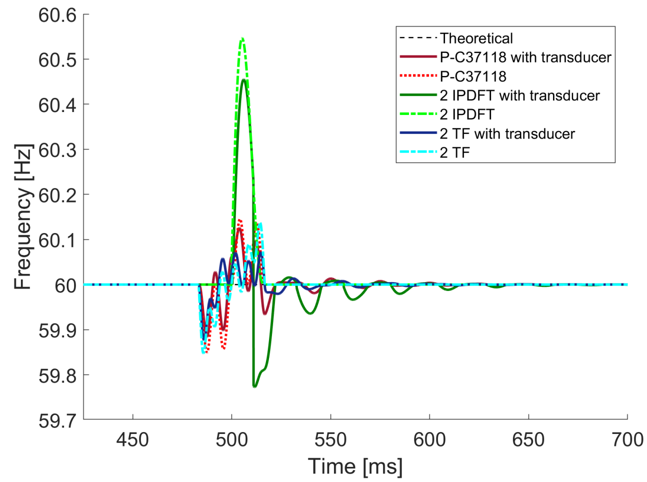

Fig. 4. Amplitude step test, frequency estimation.

TABLE II. AMPLITUDE STEP CASE: RESPONSE TIMES, OVER/UNDERSHOOT

Method		Response Time [ms]		Over/Undershoot [%]
Name	*With Transducer*	*TVE*	*Frequency*	
P-C37118	yes	19.17	93.42	0.44
	no	18.75	32.33	0.00
2 IPDFT	yes	17.33	135.17	0.78
	no	17.00	15.67	0.00
2 TF	yes	14.17	82.42	6.79
	no	14.58	33.33	6.67

analyzing the response to the phase step test signal. The comparison with Fig. 2 shows that the peak amplitude is smaller, but the oscillations are larger and their damping is considerably slower.

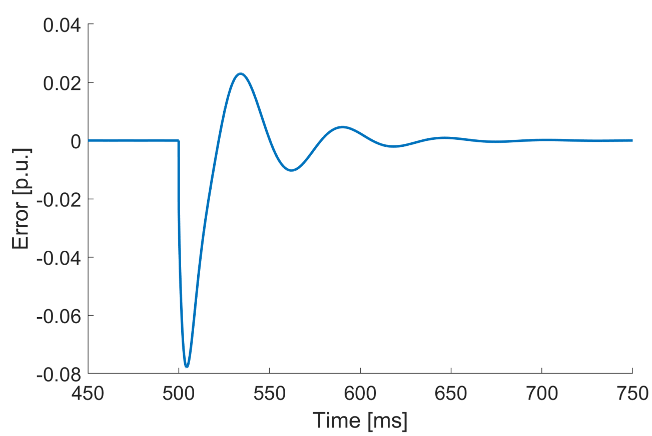

Fig. 5. Phase angle step test, deviation between actual and reconstructed primary voltage.

The impact of the CVT is even higher when the phase angle step test is considered, as it can be clearly noticed in Fig. 6, which reports the phase angle estimation error for all the algorithms with and without considering the transducer dynamics. In this case, the measurements obtained with the 2 TF, 2 IPDFT and P-C37118 show noticeable underdamped oscillations.

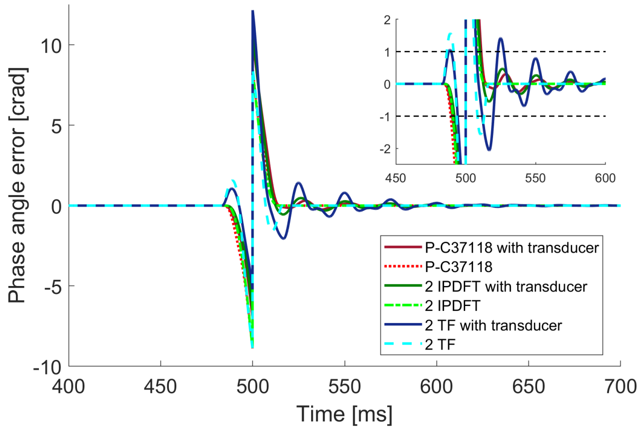

Fig. 6. Phase angle step test, phase estimation error.

The standard limit for the TVE (1 %) is also translated into phase angle error limits and reported in the zoomed inset figure, making more evident the strong impact of the CVT in the phase angle measurement after the step instant.

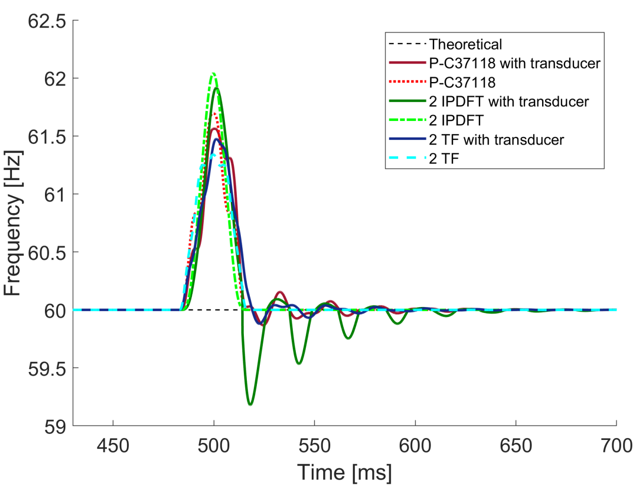

Fig. 7. Phase angle step test, frequency estimation.

Table III summarizes the step response parameters and shows that, in this case, also TVE response times increase significantly. In fact, the large oscillations due to the modes of the CVT result in a TVE that repetitively exceeds the 1% steady-state limit. As a result, even the overshoot/undershoot values rise significantly for all the methods, thus highlighting the relevance of the dynamic response of the CVT in the overall performance of the measurement chain. Frequency response times are much larger (up to six times or more, see also Fig. 7) when the CVT model is included with respect to those obtained by considering an ideal transducer. Even in this case, the ringing produced by the CVT dynamic behavior makes that the frequency measurement response time related to the PMU estimation technique is not determinant to evaluate the capability of the whole monitoring system. The dynamic description is thus the result of the combination of the CVT and PMU and even if the specifications of a PMU were complete and detailed in terms of standard test outcomes (which is not typically the case), they could be misleading in practical conditions and their usefulness from an application perspective could be not significant.

TABLE III. PHASE ANGLE STEP CASE: RESPONSE TIMES, OVER/UNDERSHOOT

Method		**Response Time [ms]**		**Over/Undershoot [%]**
Name	*With Transducer*	*TVE*	*Frequency*	
P-C37118	yes	22.92	165.67	1.74
	no	22.00	31.42	0.00
2 IPDFT	yes	21.75	201.92	3.18
	no	18.92	29.33	0.00
2 TF	yes	41.42	148.33	11.83
	no	28.00	32.50	8.98

IV. CONCLUSIONS

The paper discusses the effects of CVTs, namely the most common voltage transducers in high-voltage grids, on the dynamic response of PMU-based measurements. Their impact on amplitude and phase step tests ruled by the standard [1] have been investigated. The ideal step signals have been applied to a proper dynamic model of the CVT, and the resulting outputs have been processed by using three different, well-known PMU algorithms to estimate synchrophasor and frequency.

Results highlight how the dynamic response of the transducer cannot be neglected since it strongly affects the estimations. Frequency measurements are particularly sensitive to the transducer behavior, and the presented analysis proves that the conventional PMU standalone characterization under the standard compliance test conditions might even be misleading when considered representative of the measurement result. Response times, in particular, can vary significantly when the whole measurement chain is considered and the presented results seem promising to foster further research on PMU testing from an actual application perspective.

ACKNOWLEDGEMENTS

The work of P. A. Pegoraro was partially funded by Fondazione di Sardegna for the research project "SUM2GRIDS, Solutions by mUltidisciplinary approach for intelligent Monitoring and Management of power distribution GRIDS" - Convenzione triennale tra la Fondazione di Sardegna e gli Atenei Sardi Regione Sardegna L.R. 7/2007 annualità 2017 DGR 28/21 del 17.05.2015.

REFERENCES

[1] *IEEE Standard for Synchrophasor Measurements for Power Systems*, IEEE Std C37.118.1-2011 (Revision of IEEE Std C37.118-2005), Dec. 2011.

[2] *IEEE Standard for Synchrophasor Measurements for Power Systems – Amendment 1: Modification of Selected Performance Requirements*, IEEE Std C37.118.1a-2014 (Amendment to IEEE Std C37.118.1-2011), Apr. 2014.

[3] C. Muscas and P. A. Pegoraro, "Algorithms for synchrophasors, frequency, and rocof," in *Phasor Measurement Units and Wide Area Monitoring Systems*, 1st ed., A. Monti, C. Muscas, and F. Ponci, Eds. Elsevier, Academic Press, 2016, ch. 3, pp. 21–51.

[4] P. Castello, M. Lixia, C. Muscas, and P. A. Pegoraro, "Impact of the model on the accuracy of synchrophasor measurement," *IEEE Trans. Instrum. Meas.*, vol. 61, no. 8, pp. 2179–2088, Aug. 2012.

[5] G. Barchi, D. Macii, and D. Petri, "Synchrophasor estimators accuracy: A comparative analysis," *IEEE Transactions on Instrumentation and Measurement*, vol. 62, no. 5, pp. 963–973, May 2013.

[6] G. Frigo, D. Colangelo, A. Dervikadi, M. Pignati, C. Narduzzi, and M. Paolone, "Definition of accurate reference synchrophasors for static and dynamic characterization of pmus," *IEEE Transactions on Instrumentation and Measurement*, vol. 66, no. 9, pp. 2233–2246, Sept 2017.

[7] P. Castello, C. Muscas, P. Pegoraro, S. Sulis, and S. Toscani, "Experimental characterization of dynamic methods for synchrophasor measurements," in *Applied Measurements for Power Systems Proceedings (AMPS), 2014 IEEE International Workshop on*, Aache, Germany, Sep. 2014, pp. 1–6.

[8] D. Gallo, C. Landi, M. Luiso, P. Tosato, D. Macii, and D. Brunelli, "A testbed for the experimental characterization of estimation algorithms for phasor measurement units," in *2017 IEEE International Workshop on Applied Measurements for Power Systems (AMPS)*, Sept 2017, pp. 1–6.

[9] "Transient response of coupling capacitor voltage transformers ieee committee report," *IEEE Transactions on Power Apparatus and Systems*, vol. PAS-100, no. 12, pp. 4811–4814, Dec 1981.

[10] H. J. Vermeulen, L. R. Dann, and J. van Rooijen, "Equivalent circuit modelling of a capacitive voltage transformer for power system harmonic frequencies," *IEEE Transactions on Power Delivery*, vol. 10, no. 4, pp. 1743–1749, Oct 1995.

[11] D. A. Tziouvaras, P. McLaren, G. Alexander, D. Dawson, J. Esztergalyos, C. Fromen, M. Glinkowski, I. Hasenwinkle, M. Kezunovic, L. Kojovic, B. Kotheimer, R. Kuffel, J. Nordstrom, and S. Zocholl, "Mathematical models for current, voltage, and coupling capacitor voltage transformers," *IEEE Transactions on Power Delivery*, vol. 15, no. 1, pp. 62–72, Jan 2000.

[12] L. Kojovic, M. Kezunovic, and C. W. Fromen, "A new method for the ccvt performance analysis using field measurements, signal processing and emtp modeling," *IEEE Transactions on Power Delivery*, vol. 9, no. 4, pp. 1907–1915, Oct 1994.

[13] T. Bi, H. Liu, X. Zhou, and Q. Yang, "Impact of transient response of instrument transformers on phasor measurements," in *IEEE PES General Meeting*, July 2010, pp. 1–6.

[14] E. Pajuelo, G. Ramakrishna, and M. S. Sachdev, "Phasor estimation technique to reduce the impact of coupling capacitor voltage transformer transients," *IET Generation, Transmission Distribution*, vol. 2, no. 4, pp. 588–599, July 2008.

[15] M. Tajdinian, M. Allahbakhshi, A. R. Seifi, and A. Bagheri, "Analytical discrete fourier transformer-based phasor estimation method for reducing transient impact of capacitor voltage transformer," *IET Generation, Transmission Distribution*, vol. 11, no. 9, pp. 2324–2332, 2017.

[16] D. Belega and D. Petri, "Accuracy analysis of the multicycle synchrophasor estimator provided by the interpolated DFT algorithm," *IEEE Trans. Instrum. Meas.*, vol. 62, no. 5, pp. 942–953, May 2013.

[17] J. A. de la O Serna, "Dynamic phasor estimates for power system oscillations," *IEEE Trans. Instrum. Meas.*, vol. 56, no. 5, pp. 1648–1657, Oct. 2007.